International Journal of Marine Engineering Innovation and Research, Vol. 11(1), Mar. 2026. 105-118
(pISSN: 2541-5972, eISSN: 2548-1479)

CFD Simulation of Engine Room Ventilation Systems: A Case Study of TB Hasnur 08 Tugboat Main Engine

Rhomadon Hady Siswanto[1*], Agoes Santoso[2], Sutopo Puewono Fitri[3]
(Received: 4 February 2026 / Revised: 6 February 2026 / Accepted: 10 February 2026 / Available Online: 7 March 2026)

***Abstract*—** This study is motivated by the problem of high temperature in the engine room of the TB Hasnur 08 tugboat, which can adversely affect working comfort, engine combustion efficiency, and the overall reliability of onboard machinery. Excessive heat accumulation reduces the quality of combustion air by lowering oxygen density, which may lead to incomplete combustion and decreased engine performance. Elevated temperatures also accelerate equipment degradation and negatively impact operational safety. Therefore, an effective ventilation system capable of controlling temperature and improving air circulation within the engine room is required. This study aims to design, evaluate, and validate an optimal engine room ventilation model in accordance with ISO 8861 standards. The methodology combines empirical investigation with Computational Fluid Dynamics simulations. Field data include airflow velocity, machinery heat sources, and existing ventilation conditions. Required air for combustion and heat removal was calculated and applied in five configurations: V0, V1, V2, V3, and V4, evaluating temperature distribution, pressure, and airflow patterns. Under existing conditions, temperatures range from 45.05°C to 46.05°C. Variation 1 lowers temperatures to 42.85°C–43.95°C, Variation 2 to 42.85°C–42.95°C, while Variation 3, compliant with ISO 8861, achieves 41.85°C–42.95°C. Variation 4 adds an exhaust duct, yielding 42.85°C–43.25°C. Results identify Variation 3 as most effective, and CFD reliably predicts thermal behavior under configuration changes and operational airflow optimization benefits.

Keywords—Ventilation, Airflow, CFD, Engine Room, Tugboat, ISO 8861-1998

[*]*Corresponding Author: ndhomm@gmail.com.*

I. INTRODUCTION

1.1 Engine Room Ventilation

The engine room of a vessel is a compartment housing diverse propulsion machinery and electrical equipment. This space serves as the operational hub for all systems that support vessel function. When the equipment operates, it generates substantial heat, which has the potential to elevate the ambient air temperature within the engine room.

This study is based on the TB Hasnur 08 tugboat, which experienced engine room temperatures of approximately 39–41°C under free-running conditions (without barge towing load) at 1200 rpm during sea trials. Based on this condition, it is predicted that under loaded operation (towing a fully loaded 330-ft barge), the temperature will increase due to the higher engine load. The increased engine load generates additional heat, which subsequently raises the engine room temperature through thermal radiation from the main engine to the surrounding environment within the engine room.

Engine heat is a byproduct of combustion [5] that arises in equipment and leads to elevated temperatures in the engine room [6]. The resulting temperature rise causes the surrounding air to expand, reducing the oxygen concentration (density) in the space. When the ambient oxygen available for the fuel–air mixture in the combustion process diminishes, combustion becomes less complete, culminating in a reduction of the power output delivered by the engine.

Ventilation is defined as the process of moving air from outside the room into the room to supply clean air and expel contaminated air, thereby ensuring a continuous air exchange within the space [7]. In designing an ventilation system for a room, particularly the engine room, it is essential to consider several parameters of the ventilation such as air velocity, temperature distribution, and humidity [9]. These parameters collectively influence the conditions inside the engine room.

The design of a ventilation system must consider various factors, including the size of the engine room, the type of engine, and the airflow required to ensure all components receive adequate cooling. Accordingly, the implementation of an effective ventilation system is a crucial aspect of ship operation and maintenance, capable of enhancing productivity and the service life of the engine.

Ventilation performance is vital for maritime propulsion systems. Beyond enhancing operator comfort, effective ventilation serves as a primary and auxiliary air supply to deliver clean air for the combustion process. Air that is excessively hot or contaminated can cause more severe damage to engine room components [4].

Rhomadon Hady Siswanto, Departement of Marine Engineering, Sepuluh Nopember Institute of technology, Surabaya 60111, Indonesia, ndhomm@gmail.com.
Agoes Santoso, Departement of Marine Engineering, Sepuluh Nopember Institute of technology, Surabaya, 60111, Indonesia. E-mail: agoes@its.ac.id
Sutopo Puewono Fitri, Departement of Marine Engineering, Sepuluh Nopember Institute of technology, Surabaya, 60111, Indonesia. E-mail: sutopopf@its.ac.id

Therefore, the ventilation system design must be conducted with precision to ensure a sufficient air supply while simultaneously reducing the engine room temperature.

The principal aspects of an effective engine-room ventilation system encompass cooling air and combustion air [12]. Cooling air serves to remove heat from the engine, generator, and other equipment, while combustion air is the oxygen necessary for fuel oxidation in the engine. Both air streams directly influence engine performance and the service life of the unit, and therefore must be carefully considered in the design of the ventilation system.

The importance of a well-designed ventilation system becomes increasingly evident in this context. Ventilation aims to remove heat buildup within the engine room and maintain temperatures at safe and comfortable levels [3]. Contaminated hot air must be expelled either passively or forcibly through the ventilation system, with mechanical fans functioning to supplant low-pressure air into the engine room effectively [13]. The supplied air is then directed through a purpose-built ducting system to ensure uniform airflow across the entire engine-room space. The ventilation system is not only essential for maintaining operator comfort but also for supporting the performance of equipment and machinery within the engine room [14]. [14]. Diesel engines used in ship propulsion and auxiliary machinery, such as generators, rely heavily on adequate airflow for optimal operation, effective ventilation also aims to provide air for the combustion process, maintain cool temperatures to remove hot air, and ensure that personnel can operate under safe environmental conditions [15].

In particular, ventilation within the engine room, especially on tugboats, is not regulated by regulations; however, minimum air temperature limits are provided for the engine room, as shown in Table 1.

TABLE 1
MACHINERY INSTALLATION ACCORDING NIPPON KAIJI KYOKAI (CLASSNK) PART D 1.2 [1]

Temperature	Installed Location	Temperature (°C)
Air	In Enclosed Space	0 to 45(Note)
	In Spaces exceeding 45°, or below 0°	According to specific Condition
	On the open deck	-25° to 45°(Note)
Sea water	-	32°(Note)
Note : Other temperatures deemed appropriate by the Society might be accepted in ships not intended for unrestricted service.		

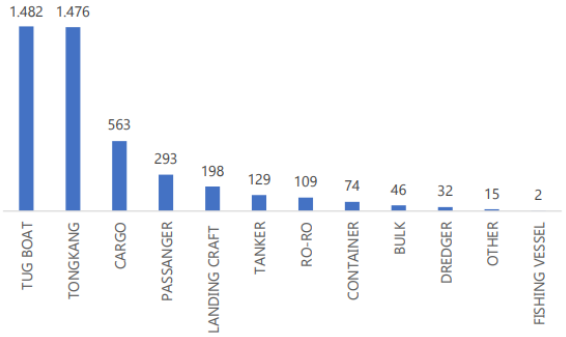

Figure 1. Number of National Sea Transportation Fleets by Vessel Type in 2019 [2]

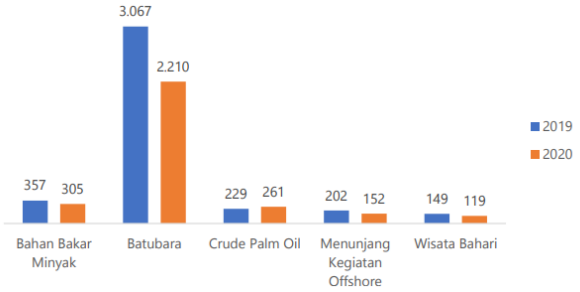

Figure 2. Graph of the Number of the National Sea Transportation Fleet by Ship Cargo Capacity up to September 2020.[2]

As a general rule [15], the minimum intake air for the engine room is approximately 1.75 times the main engine air consumption at SMCR (Safe Magnetic Curve Rating/Specified Mean Cooler Room, depending on context). Therefore, 2.0 times the main engine air consumption at SMCR may be sufficient. Additionally, the internal engine-room air must also account for the minimum environmental pressure; the pressure inside the engine room should be at least 5 mm H2O (equivalent to 0.0005 bar) above the ambient pressure outside the engine room at the outlet position located outside the funnel.

1.2 Tug Boat

A tugboat, commonly referred to as a tug, is a vessel designed to tow, push, or assist other ships in maneuvering within confined waters [16]. In performing its maneuvers, the tug is equipped with a main propulsion system (Main Engine) and auxiliary machinery (Auxiliary Engine). Due to its function, tugboats are widely employed in offshore activities as well as operations in port environs [17].

Tugboats are generally not very large in size; this class of vessel has a distinctive low-slung hull and is equipped with a powerful engine. Based on these characteristics, tugboats serve to perform the following functions:

- Maneuvering: Tugboats assist larger vessels in maneuvering, such as docking or undocking at ports, turning in confined waters, or tracing a difficult passage.
- Towing: Tugboats are also employed to tow or assist vessels that cannot sail under their own power, such as damaged or incapacitated ships.
- Assistance: Additionally, tugboats provide support in various emergency situations, including firefighting, search and rescue, or salvage operations for grounded or stranded vessels.

As illustrated in Figures 2 and 3, maritime operations in Indonesian waters are predominantly characterized by tug boats. These vessels are extensively utilized for towing coal barges from mining areas dispersed throughout the Indonesian archipelago to mother vessels or directly to coal-fired power plants (PLTUs), conducted either through estuarine transshipment operations or direct transportation routes. In general, the primary propulsion engine used on tugboats is a diesel engine. A portion of the fuel consumed by the engine is lost to the environment as heat, which is radiated or released into the surrounding air within the engine room [12]. Moreover, heat arising from generator inefficiency and exhaust-pipe losses can readily be comparable to the heat radiated by the engine. Elevations in temperature caused by these heat releases can significantly affect operational continuity, maintenance requirements personnel safety, switchgear apparatus, and the performance of the engine or generator units.

The machinery systems of tugboats, including towing tugs, push tugs, and assisting tugs, are generally characterized by similar machinery configurations. The principal distinction among these types of tugboats lies in their propulsion systems.

TABLE 2.
LIST OF PREVIOUS RESEARCHER

no	Title	Author	Year	Content	Main Refference
1	An Investigation of the Effect of Ventilation Inlet and Outlet Arrangement on Heat Concentration in a Ship Engine Room	[3]	2004	An analysis of heat within the engine room of a warship, conducted by performing CFD modeling to assess the existing distribution of air flow.	Using CFD as a method for modeling airflow and heat distribution within the engine room
2	Computational fluid dynamics analysis of engine room ventilation of a bulk carrier plying in the inland waterways of Bangladesh	[4]	2018	Factors contributing to effective engine room ventilation on bulk carriers; based on ISO 8861:1998, the inlet duct diameter and the air flow rate (air change per hour) are two main factors in engine room ventilation. Temperature rise in the engine room is caused by inadequate air flow. CCM is used as a numerical analysis tool, and CFD is used for modeling; modeling the ducting diameter influences air velocity and its relation to heat within the engine room	Heat calculations for each equipment within the machinery can be performed using ISO 8861; CCM is used as a numerical analysis tool, and CFD is employed to model airflow and heat within the engine room
3	The Air Flow Analysis in Engine Rooms at Frigate Class Ship with CFD Approach (Computational Fluids Dynamics)	[6]	2018	High engine room temperatures in frigate-class ships, after repowering the engine, ranged from 60 to 65°C. Therefore, CFD simulations are required to reduce the engine room temperature. The study found that the initial airflow was 28,250 m^3/h, and to achieve an optimal temperature it was adjusted to 57,555.69 m^3/h."	Changes in the air supply to the engine room will affect the temperature within the engine room; CFD is used to simulate airflow inside the engine room
4	Design and Research of Marine Nuclear Power Platform Engine Room Ventilation System	[8]	2020	Principle of ventilation in a nuclear-powered offshore platform building. In this study, the diesel engine room ventilation system is used as an example, where the design methods for ventilation systems commonly employed on offshore platforms and ships are introduced, and the total ventilation rate required to ensure performance is calculated at full load, so that the ventilation on the nuclear-powered platform.	Ventilation is used to remove heat from inside the room and to provide combustion air for engines and machinery.
5	CFD simulation of the ventilation system and air control for the COVID-19 isolation room on the 750 DWT	[10]	2021	Analysis of the Covid-19 isolation space on a vessel, consisting of an analysis of airflow characteristics and performance in the ventilation system	The use of CFD as a method to determine the characteristics and performance of air flow.
6	Investigating the Thermal Profile of a Marine Vessel Engine Room through Simulation with Field Measurements	[11]	2014	Evaluation of CFD usage to model ventilation on ships under extreme conditions, specifically in Arctic regions, with improvements to the ventilation system that can enhance engine and generator set efficiency and reduce the temperature range to improve thermal comfort.	CFD usage, compared to data-driven models, indicates a temperature difference of about 0.4%. CFD can be utilized in the design phase for optimizing the engine room system.

1.3 CFD

In an era of advancing technology, the use of simulation methods such as Computational Fluid Dynamics (CFD) can also be employed to analyze and optimize the design of ventilation systems [11]. Through CFD modeling, one can obtain deep insights into the airflow and temperature distribution [10] within the engine room. The results of these simulations can assist engineers in designing ventilation systems that are more efficient and effective.

Moreover, CFD is effective for design analysis in engineering; many researchers [18] [19] [20]utilize CFD as a tool for performance evaluation, airflow characterization, and system optimization.

TABLE 3
MAIN ENGINE AND AUXILIARY DATA

No	Brand	Manufacture	Cyl	Hp	Rpm	Year	Model	Series	Position
1	Yanmar	Yanmar Co. Ltd	12	1100 Hp	1800	2010	12LAK STE 2	0803	PS
2	Yanmar	Yanmar Co. Ltd	12	1100 Hp	1800	2010	12LAK STE 2	0802	SB
3	Weichai	Weifang - Weichai	4	68	1500	2	TD226B-CD1	2231	PS
3	Weichai	Weifang - Weichai	4	68	1500	2	TD226B-CD1	2244	SB

1.4 State of the art

The application of CFD analysis to airflow in order to obtain optimal engine room temperatures has been implemented in several previous studies, including applications on cargo vessels [21], naval warships [6], and Landing Ship Tank (LST) vessels [22]. In the present study, CFD is applied to a coal-towing tugboat operating under full-load (laden) conditions.

The novelty of this study lies in the development and optimization of an engine room ventilation model for the TB Hasnur 08 tugboat using Computational Fluid Dynamics (CFD) in accordance with ISO 8861. This study systematically evaluates multiple ventilation configurations (V0–V4) to determine the most effective design for improving airflow distribution and reducing engine room temperature under realistic operating conditions. The analysis focuses on the operational speed of the tugboat TB Hasnur 08 while towing a coal barge with comparisons of temperature, pressure, and air velocity profiles within the engine room. Variations in airflow velocity are applied to evaluate changes in engine room air pressure and temperature under both actual and modified conditions. The ISO 8861 standard is used as a reference for determining the applied airflow velocities.

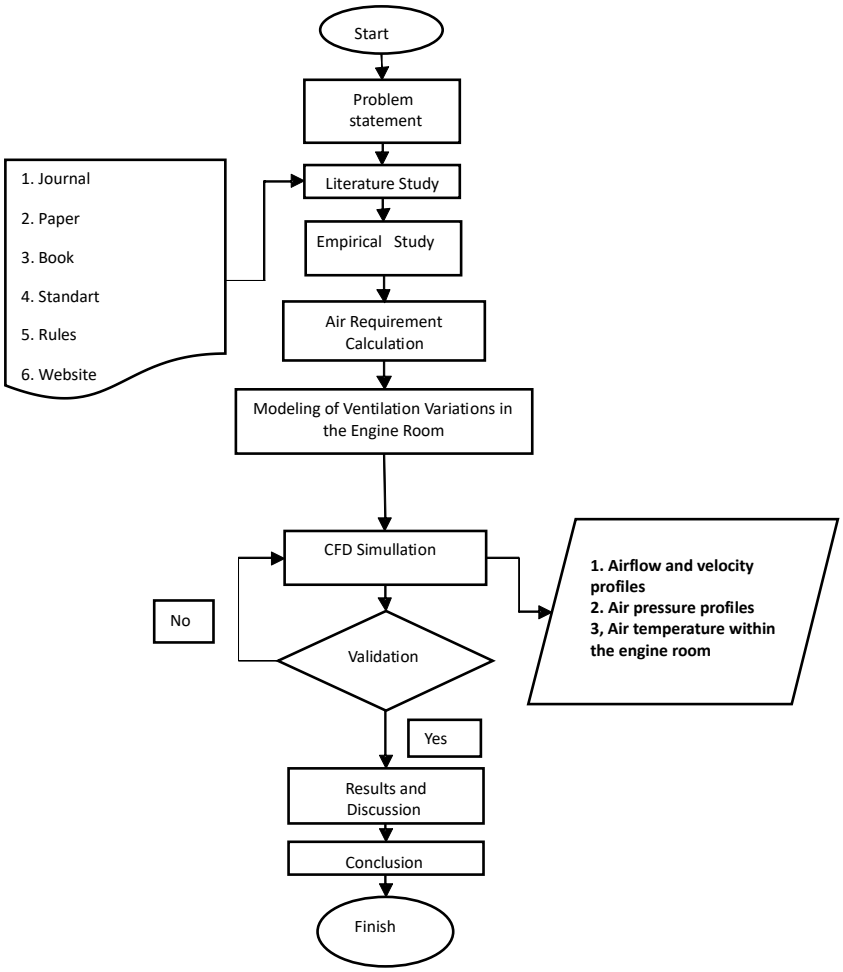

Figure 3. Research flowchart

1.5 Problem statement and research objectives

a. Problem Statement

Based on the identified background issues of the tugboat TB Hasnur 08, the research problems are formulated as follows:

- How can an optimal ventilation system model be designed to improve efficiency and operational comfort within the engine room of the tugboat TB Hasnur 08?

- How does the thermal performance of the proposed ventilation system design perform in the engine room of the tugboat TB Hasnur 08?

b. Research objective.

Based on the defined problem formulation, the objectives of this study are as follows:

1. To develop an optimal ventilation system model for the engine room of the tugboat TB Hasnur 08, in accordance with ISO 8861, ASHRAE Standard 15, and BKI Classification Rules, Volume III: Rules for Machinery Installation.
2. To perform numerical simulations to analyse and evaluate the performance of the engine room ventilation system using the Computational Fluid Dynamics (CFD) method. The evaluated performance parameters include air temperature distribution, airflow velocity profiles, and air pressure within the engine room of the tugboat TB Hasnur 08

II. METHOD

2.1 Research flow chart

The research methodology serves as the fundamental framework guiding the execution of the study. It comprises a series of planned activities aimed at analyzing and addressing the problems under investigation. The research process is conducted through several stages, including problem formulation, literature review, data collection, modeling, simulation, data validation, and conclusion drawing. Each stage is designed to ensure the accuracy of the research outcomes and to provide a significant contribution to the understanding of the studied issues, thereby producing findings that are valid and applicable in practical contexts.

2.2 Empirical study

In this stage, data are collected comprehensively for the tug TB Hasnur 08. In addition to the main vessel data, air velocity measurements inside the tug TB Hasnur 08's engine room are also undertaken.Data utama kapal

a. Main data

TB Hasnur 08 is a tugboat with a Length Over All (LOA) of 27 m, LPP of 25.5 m, and moulded beam of 8.2 m, with the main engine and auxiliary engine details provided at table 3.

The engine room is located in a space below the main deck, positioned between frame 16 and frame 34. Inside this space are the main engine and auxiliary engine, along with several other machinery and piping.

During operation under existing conditions, the air velocity inside the engine room was measured. The airflow velocity was generated by the mechanical fan.

The air velocity inside the engine room of TB *Hasnur 08* was measured at each side of the engine room. The measured air velocity data were then used as the airflow velocity settings for each variation in the CFD simulations. The results of the air velocity measurements are presented in Table 4. Based on the results of field measurements on the tugboat TB *Hasnur 08*.

Based on the results of field measurements on the tugboat TB *Hasnur 08*, the average air supply provided by the forced ventilation system was 36.02 m^3/s.

TABLE 4
AIR SPEED VARIATION (BOUDARY CONDITION)

Name of Variation	Supply ME P (m/s)	Supply AE P (m/s)	Supply ME S	Supply AE S	Additional Vent P	Additional Vent P
Existing supply Variasi 0 (V0)	8,44	6,38	12,52	10,7	-	-
Variasi 1 (V1)	15	12	15	12	-	-
Variasi 2 (V2)	20	15	20	15	-	-
Variasi 3 (V3)	26,75	20	26,75	20	-	-
Variasi 4 (V4)	26,75	20	26,75	20	1,5	1,5

TABLE 5.
PROPERTIES OF FLUID

Properties of fluid	Number
Inlet temperature (C)	36,5
ρ Density (kg/m^3)	1.146
cp Heat spesific (kJ/kg.K)	1007
k Thermal Conductivity (W/m.K)	24,2 e-03
μ Absolute viscosity ($N.s/m^2$)	1,9022 e-05

b. Main Engine Heat Data

Heat generated by the main engine is taken from several components, namely the heat exchanger, turbocharger, exhaust gas pipe, and the main engine block. The heat extraction from these components is based on the existing condition that these areas are the highest heat-release points contributing to the engine room temperature.The heat exchanger in the main engine is the primary location for circulating the cooling liquid. The cooling liquid used is a specialized fluid, commonly referred to as water coolant, which functions to absorb heat from several parts of the main engine (Gilbert Gedeon 2009). This fluid is pumped to enhance the effectiveness of heat transfer from the lubricating oil, liners, and cylinder head., the highest recorded temperatures are taken from the measurement data, with

the maximum values being 89.1°C on the left main engine side and 88.2°C on the right engine. The turbocharger is a turbine device that enhances internal combustion efficiency and engine output by compressing the air entering the combustion chamber [23]. From the heat measurements of the main engine turbocharger, the portside positions recorded 345.9°C on Bank 1 and 385.4°C on Bank 2, while the starboard side recorded 372.4°C on Bank 1 and 391.1°C on Bank 2. Because the hot air is utilized, the turbine heat is conducted to the entire turbine surface. Typically, turbines are provided with heat insulation material; however, for the investigated vessel TB Hasnur 08, no thermal insulation was used, resulting in very high radiative heat transfer from the turbine into the engine room. In addition, air measurements in the exhaust were conducted only for the exhaust gases inside the engine room. From the measurements on the left engine, Bank 1, Point 1 = 57.1°C; Point 2 = 56.9°C. Bank 2, Point 1 = 72.3°C; Point 2 = 70.9°C. For the right engine, Bank 1, Point 1 = 61.7°C; Point 2 = 60.8°C. Bank 2, Point 1 = 72.7°C; Point 2 = 72.7°C. For the exhaust gas pipes located on the left and right funnel, the measured values vary between 53°C and 55°C. To simplify the heat simulation boundary, 55°C was taken as the limit. maximum turbocharger temperature, 189.3°C.For the heat exchanger on the auxiliary engine, temperatures range from 56.6°C to 61.4°C, and the temperature used in the simulation for the heat exchanger is 61.4°C. The alternator windings, as the electrical power source, dissipate heat during operation in the range of 37.8°C to 53.2°C.The exhaust gas temperature measurement from the left engine yielded the highest average value among the measurements. This is because the auxiliary engine operated at a constant RPM of 1500 rpm. The measured temperature of the exhaust gas pipe is 51.7°C, while the exhaust gas temperature for the right engine is 28°C. In addition to measurements at these three locations, heat measurements were also taken on the exhaust pipe that passes through the engine room. This exhaust pipe measurement was divided into five sections, with each section having a length of 1 meter. The exhaust pipe passing through the engine room has a diameter of 60 mm and is insulated with glass wool and wrapped with a zinc layer on the outside. The measured heat refers to the surface temperature of the zinc outer wrapping of the exhaust pipe.

c. Heat from electrical equipment

The heat generated by electrical equipment in the engine room of the tug TB Hasnur 08 originates from energy consumption by the lighting and the Main Switch Board (MSB). The lighting in the engine room consists of two types of lamps: Fluorescent Lamp (FL) 2x18 W in tubular form, widely known as neon lamps, and 400 W spotlights. Lighting installations in the engine room comprise 10 FL lamps and three 400 W spotlights, with three units of each. The total thermal load is produced by heat conduction and convection through the electrical wiring installations and the room's air circulation.

The heat produced by the installed neon lamps during measurements is not significant; the radiated heat is measured to be in the range of approximately 34–36°C. In contrast, the spotlights installed in the engine room generate temperatures around 50–55°C. These spotlights are used as the primary lighting source for the main engine, while another unit is used to illuminate the main control panel. When the spotlights are on, the radiated heat they produce affects the temperature inside the engine room of the tug TB Hasnur 08.

The generator produces 50 kW of electrical power, while during cruising the generator load ranges from 28 to 36 kW. The unused portion of power is converted into heat in the busbars or copper conductors, and this heat is subsequently released into the surrounding environment, namely the engine room. From the heat measurements on the Main Switch Board (MSB) at the front and rear sections, the average value is 39°C.

d. Heat from other equipment

HPU (Hydraulic Power Unit) is one of the main components of the ship's steering system (Steering Gear System). This device consists of a pump and a reservoir connected to the rudder mechanism; the rudder blades are subsequently operated through a hydraulic circuit. The steering motion can be driven by an electric (electro-hydraulic) system or by a manual mechanism. In electric mode, the pump is activated by a switch/solenoid that routes high-pressure fluid to shift the rudder to the left or right. When the vessel turns, the fluid is driven to deliver power to the steering actuator; when the vessel is straight, the fluid circulates back from the system to the HPU reservoir. maneuver responses at numerous bends and turns. From the heat measurements, the temperature fluctuates between 40–42°C, with the HPU temperature taken to be approximately 41.7°C.

2.3 Air requirement calculation (ISO 8861)

The next stage involves calculating the air demand in the engine room of the tug TB Hasnur 08 based on ISO 8861 standards. The air requirement inside the engine room serves to support combustion and to reduce heat emissions within the engine room of TB Hasnur 08. In general, ISO 8861 divides the air demand inside the engine room into two categories: the air required for combustion and the air required for heat evacuation. This broad formulation is defined by ISO 8861 as follows:

In general, ISO 8861 divides the air demand inside the engine room into two categories: the air required for combustion and the air required for heat evacuation. This broad formulation is defined by ISO 8861 as follows:

$$Q = q_c + q_h \quad (1)$$

With Q representing the total air capacity for the engine room, qc representing the air requirement for combustion, and qh representing the air requirement for heat evacuation.

The total air demand for combustion is the sum of the air demand for the main engine (qdp), the air demand for the diesel generator (qdg), and the air demand for the boiler (qb). Since TB Hasnur 08 does not have a boiler, qb can be considered zero (0). The main engine used is a 12LAK STE2 with a power of 809 kW, and the auxiliary engine has a power of 50 kW. From the air-flow

requirement equation for the main engine, qdp = 2.863717 kW, and the air demand for the auxiliary engine is qdg = 0.088496 kW. The requirement for combustion for the main engine and the generator is 2.952 m³/s.

The air demand for evacuating heat released by equipment, both the main propulsion machinery and the auxiliary machinery, as well as electrical equipment (qh), is calculated to determine the exact aircapacity required by the engine room beyond the air needed for combustion. This air is used as a heat transfer medium. From Equation 5, qh = 83.543 m³/s.

2.4 CFD Simullation

In Geometry 1 (figure 5 (a)), simulations were conducted for Variation 0, Variation 1, Variation 2, and Variation 3. Variation 0 corresponds to the initial measurement values. Variation 1 and Variation 2 represent the air speeds obtained from measurements of other TB Hasnur fleet vessels. Variation 3 corresponds to the ISO 8861-based calculation. Variation 4 uses Geometry 2 that show in figure 5 (b) and applies air speeds calculated according to ISO 8861; the difference between Variations 3 and 4 is the presence of exhaust air with a velocity of 1.5 m/s. There are no changes in ducting dimensions across the air-speed variations; the variations focus solely on the air speeds from V1 to V4.

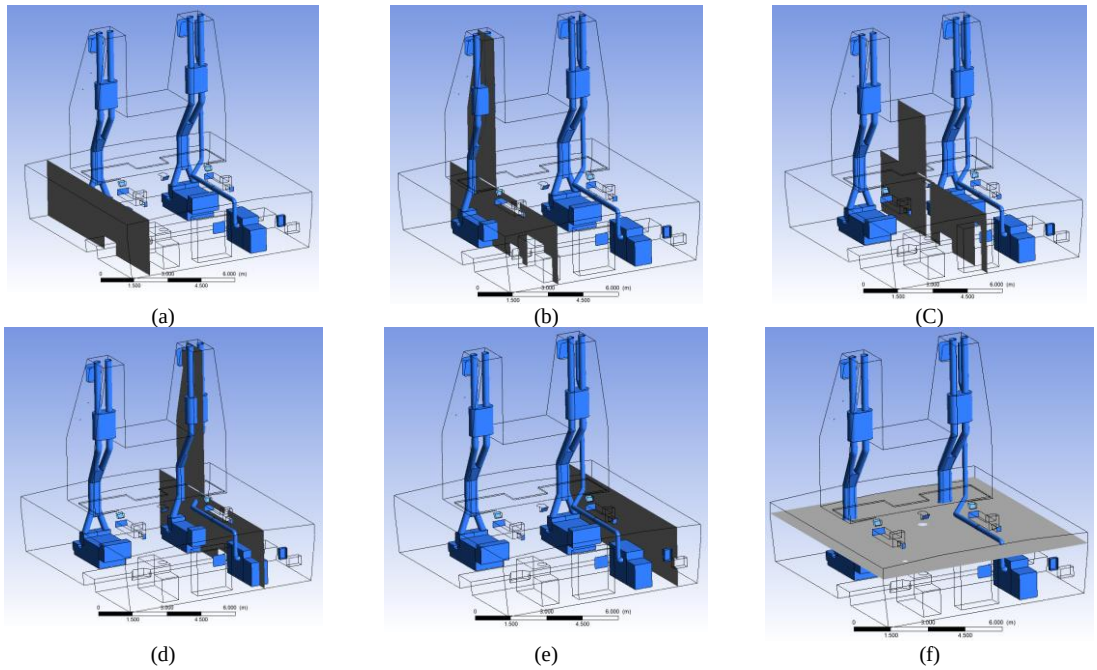

Figure 5. (a) A observation area at the starboard side of the engine room (b) B observation area at the starboard engine (c) C observation area at the center of the engine room (d) D observation area at the port engine (e) E observation area at the port side of the engine room (f) F observation area of temperature at a height of 300 mm above the deck

TABLE 6
AIR VELOCITY VARIATION 0

V0	Supply ME P	Supply AE S	Supply ME S	Supply AE S
V (m/s)	8,44	6,38	12,52	10,7
A (m^2)	1,009	0,255	1,822	0,284
Q (m^3/s)	8.52	1.63	22.82	3.05

TABLE 7
AIR VELOCITY VARIATION 1

V0	Supply ME P	Supply AE S	Supply ME S	Supply AE S
V (m/s)	15	12	15	12
A (m^2)	1,009	0,255	1,822	0,284
Q (m^3/s)	15,14	3,06	27,34	3,42

The fluid flowing into the engine room is air with properties as listed in Table 7.

2.5 Observation area

Simulations of the TB Hasnur 08 tugboat engine room area were conducted using Ansys 2025 R1. The final results of the simulations are obtained at the post-processing stage after the iterations, yielding distributions in contour maps of velocity, temperature, and air pressure inside the engine room. These contours can be presented as visual images or as numerical data. The observation area is shown in Figure 5. Contours displayed correspond to the X-axis (x/l), Y-axis (y/h), and Z-axis (z/w). The qualitative data consist of visualized distributions of temperature, velocity, and air pressure in the observation area.

Observation Area A is Starboard hull side area along the engine room, from the rear bulkhead at Frame 16 to the front bulkhead at Frame 34, from the lower wall up to the main deck. The distance from the centerline of the ship is x/l = +3.55 meters (positive values indicate the right direction). Observation Area B is the midsection through the Starboard main engine from the rear bulkhead at Frame 16 to the front bulkhead at Frame 34; the lower boundary is the floor and it extends upward, cutting the right-hand funnel. The distance from the centerline is x/l = +2.17 meters. Observation Area C is the midship region at x/l = 0 meters, from Frame 16 to Frame 34 inside the engine room; the upper boundary lies at the engine room floor, while the upper boundary follows the shape of the funnel junction. Observation Area D is the same position as Area B but at x/l = -2.17 meters (negative values indicate the left direction) portside main engine. Observation Area E is the same as Area A but at x/l = -2.55 meters (negative values indicate the left direction) Portside hull. The Area F is the observation area at a height of 300 mm bellow the main deck, and its intersection extends throughout the entire engine room.

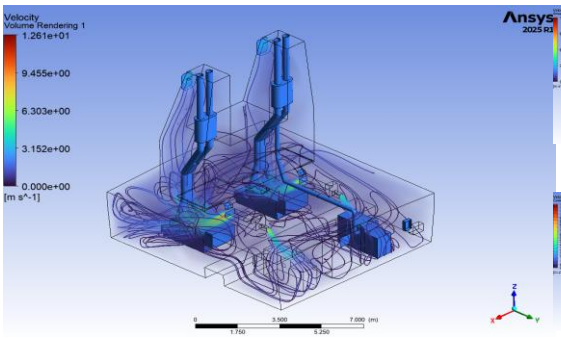

Figure 6 Air speed inside engine room Variation 0

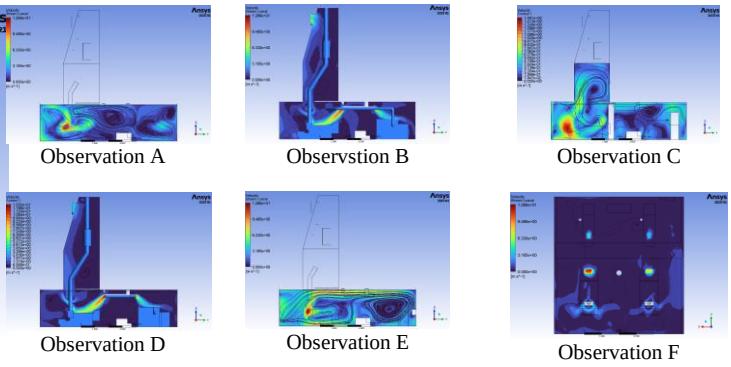

Figure 7. Air velocity at observation area Variation 0

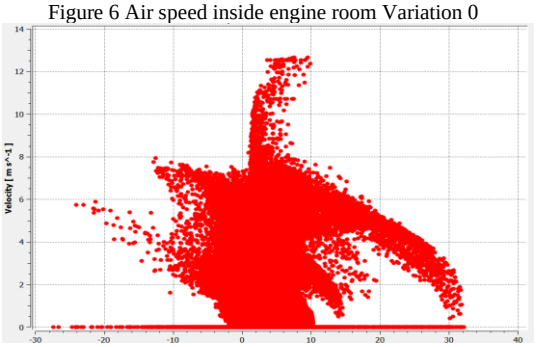

Figure 10 Air velocity and pressure chart Variation 0

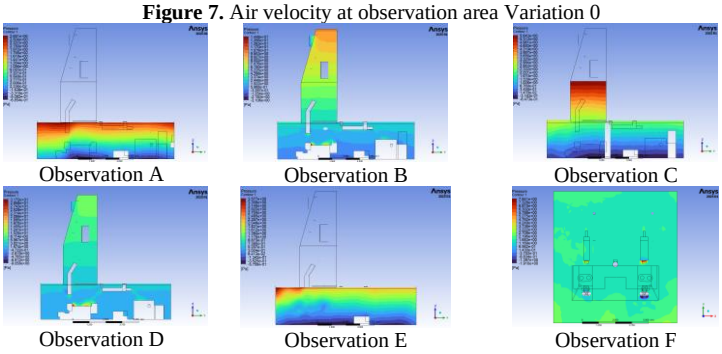

Figure 8. Pressure at observation area Varition 0

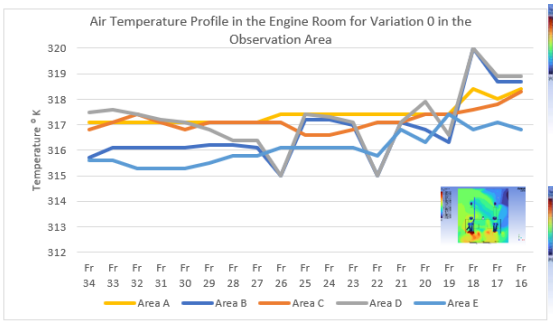

Figure 11. Temperature observation at frame Variation 0

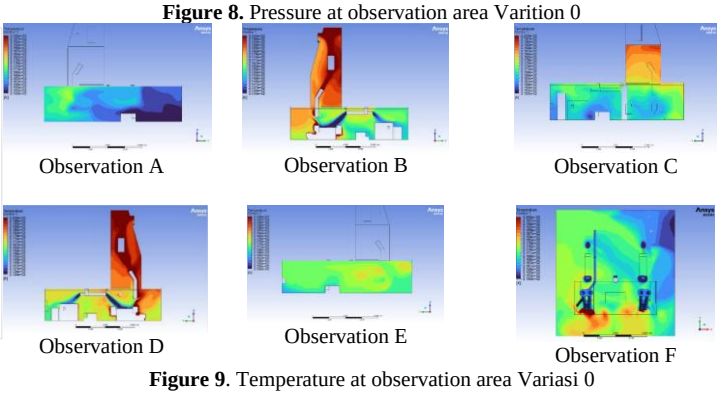

Figure 9. Temperature at observation area Variasi 0

III. Results and Discussion

3.1 Result from Variation 0

Variation 0 simulation represents the existing condition (Table 6), in which the inlet air velocity supplied to the engine room is set to the actual operating value. The air velocity used in this simulation is obtained from field measurement results. This simulation describes the airflow pattern within the engine room of the tugboat TB Hasnur 08.

Based on the measured air velocity data and the ducting dimensional data, the total air supply capacity delivered into the engine room was calculated to be 36.02 m³/s. “The measured ventilation ducting capacity under existing conditions is lower than the capacity calculated based on the ISO 8861 standard. The air supplied by the ventilation system accounts for only 0.416 (41.6%) of the required airflow determined by the calculation.

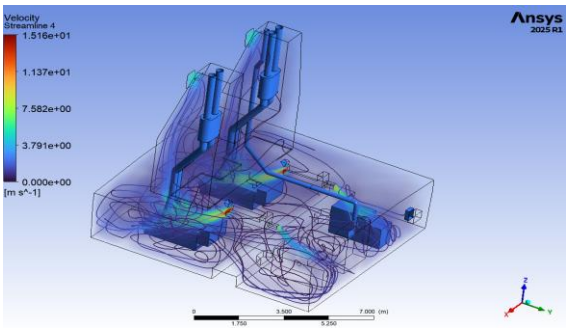

Figure 12 Air speed inside engine room Variation 1

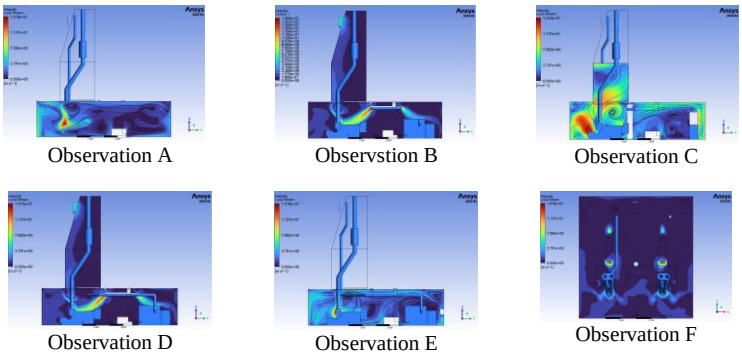

Figure 13 Air velocity at observation area Variation 1

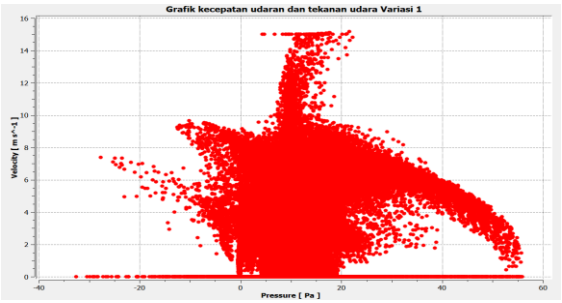

Figure 16 Air velocity and pressure chart Variation 1

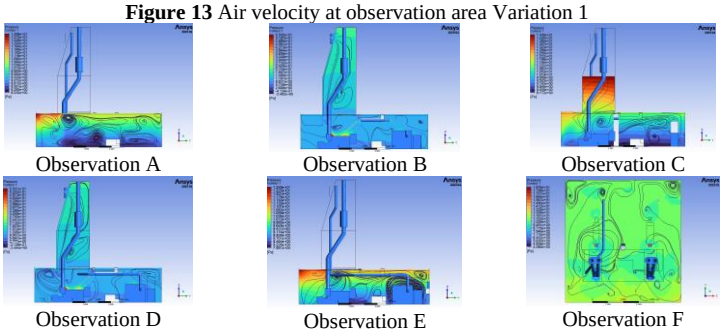

Figure 14 Pressure at observation area Variation 1

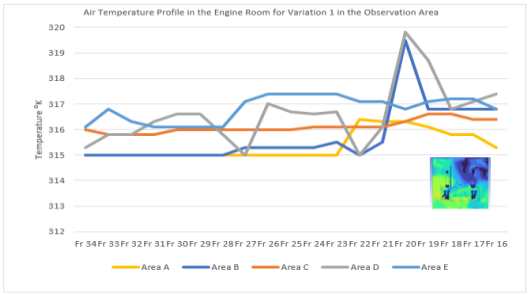

Figure 17 Temperature observation at frame Variation 1

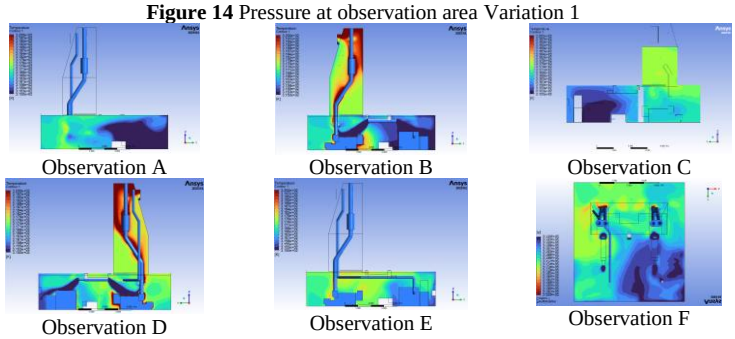

Figure 15 Temperature at observation area Variation 1

The simulation results for Variation 0 indicate that the air pressure inside the engine room ranges from –27.346 Pa to 32.177 Pa. The occurrence of negative pressure in several areas of the engine room indicates a pressure reduction relative to the standard atmospheric pressure of 1 atm (101,325 Pa). This pressure reduction predominantly occurs in the lower part of the engine room, caused by the airflow supplied by the mechanical fans forming vortices in the upper region due to interactions and impingement with engine structures. In addition, a pressure drop is also identified in the tubular exhaust gas duct area. The highest air pressure within the engine room occurs in the vicinity of the main engine, on both the portside and starboard sides, particularly at bends and curved sections at the engine ends that directly interact with the airflow. The average air pressure profile within the engine room ranges from 2 to 14 Pa. This pressure increases toward the upper region of the engine room, reaching the natural ventilation system, which functions as the outlet pathway for air discharge from the engine room.

TABLE 8
AIR VELOCITY VARIATION 2

Variation 2	Supply ME P	Supply AE S	Supply ME S	Supply AE S
V (m/S)	20	15	20	15
A (m^2)	1,009424	0,2552	1,822912	0,28462
Q (m^3/s)	20,19	3,83	36,46	4,27

The air temperature distribution shown in Figures 9 (b),(d) indicates that heat removal by airflow under the existing condition causes the air to accumulate at frame 16/17 and become trapped in the upper region, particularly at the junction between the bulkhead and the main deck. Consequently, the air temperature at that location ranges from 318.2 K to 319.2 K (45.05 °C–46.05 °C). The temperature predicted by the simulation is close to the actual conditions measured inside the engine room.

3.2 Result from Variation 1

Variation 1 represents a condition that is largely similar to Variation 0; however, the inlet air velocity is increased in accordance with Table 7. The air velocity

values are adopted from measurements of other tugboat fleets and rounded to simplify the simulation process for Variation 1.

The increased air velocity was multiplied by the ducting cross-sectional area, which remains based on the existing condition of the engine room, to obtain the air supply capacity used in the Variation 1 simulation. The resulting airflow capacity supplied to the engine room during the simulation is approximately 48.96 m³/s. However, the total supplied airflow in Variation 1 remains below the total airflow capacity calculated according to ISO 8861, with the simulated capacity corresponding to 0.56 (56%) of the calculated requirement.

An increase in air velocity affects the volume of air supplied into the engine room per second, leading to a rise in the internal air pressure. As shown in Figures Figure 13 (b) and (d) the air velocity in Variation 1 is higher than that in Variation 0. At the duct outlet, the maximum air velocity reaches approximately 15.02 m/s and then gradually decreases along the flow path.

The air pressure inside the engine room continuously increases as the air supply is consistently delivered into the space. In addition to the increased air velocity, the simulation results for Variation 1 indicate a corresponding increase in air pressure.

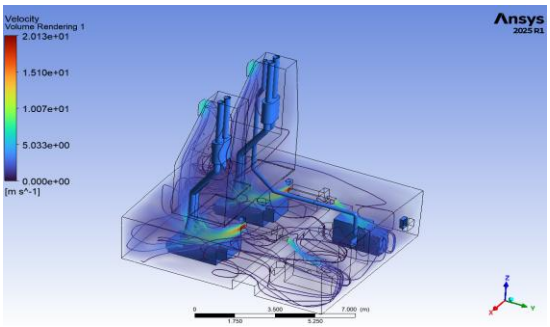

Figure 18 Air speed inside engine room Variation 2

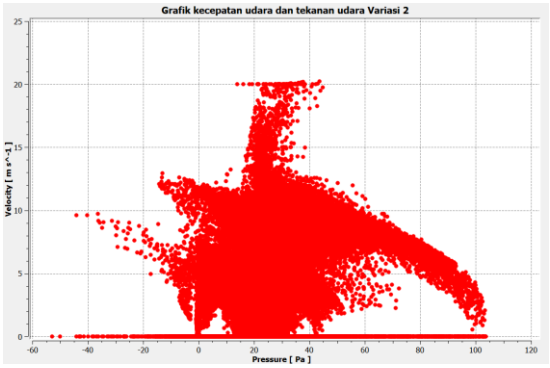

Figure 22 Air velocity and pressure chart Variation 2

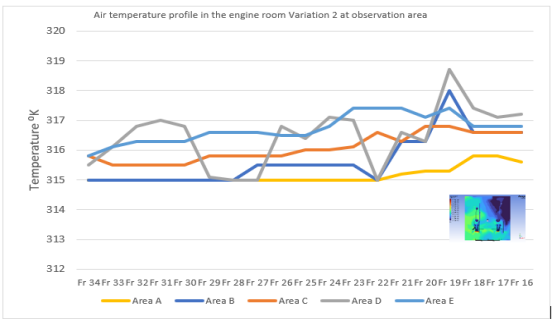

Figure 23. Temperature observation at frame Variation 2

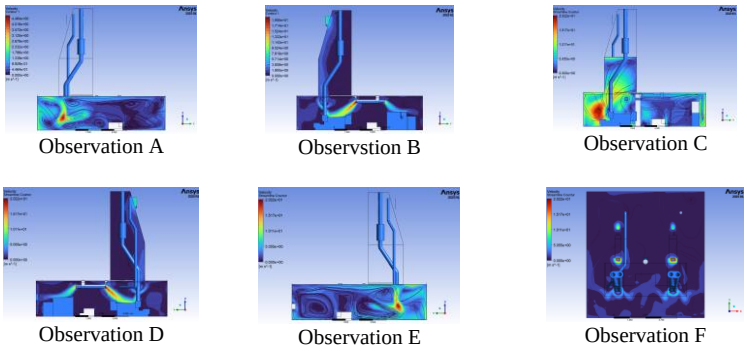

Figure 19. Air velocity at observation area Variation 2

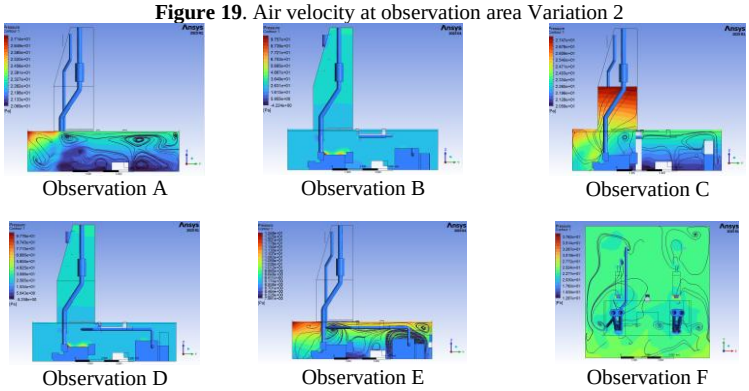

Figure 20. Pressure at observation area Varition 2

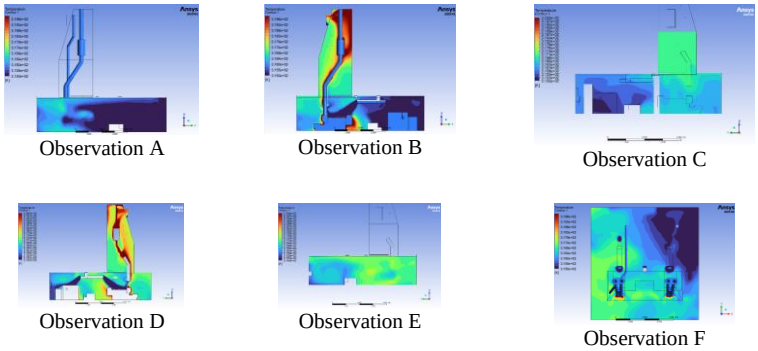

Figure 21. Temperature at observation area Variasi 2

At higher air velocities, the lower region of the engine room and the cylindrical exhaust gas area also experience greater pressure reductions. This phenomenon occurs because the increased airflow velocity intensifies the formation of pressure drops. In Observation Area A, located near the wall, the maximum air pressure is observed at the ends of Frame 16 and Frame 17, with an increase of approximately 12.98 Pa, while the lowest pressure in this area occurs in the lower region with a recorded value of 8 Pa.

As shown in Figures 14 (b) and (d), the highest pressure is identified in areas where the airflow impinges on operating machinery, reaching approximately 55 Pa. In contrast, the louvre area exhibits a pressure drop to –

3.945 Pa. The negative pressure in this region is caused by the pressure difference between the external ambient air at 1 atm and the pressurized air inside the engine room, resulting in an outward airflow driven by a pressure difference of 3.945 Pa.

In the central area, as illustrated Figure 14 (c), the airflow continues to move upward and experiences a pressure increase of up to 14.58 Pa, while in the lower region the pressure decreases to approximately 8 Pa. The airflow induced by Variation 1 results in an increase in air pressure within the engine room, accompanied by a greater magnitude of pressure reduction in certain areas. The air pressure inside the engine room ranges from –26.22 Pa to 55.743 Pa. The overall increase in pressure throughout the engine room promotes a faster airflow toward the natural ventilation system, facilitating the discharge of air out of the vessel.

TABLE 9
AIR VELOCITY VARIATION 3

Variation 3	Supply ME P	Supply AE S	Supply ME S	Supply AE S
V (m/S)	26,75	20	26,75	20
A (m^2)	1,009424	0,2552	1,822912	0,28462
Q (m^3/s)	27,00	5,10	48,76	5,69

Based on the interpretation of Figures 16, the air pressure within the engine room generally operates in the range of 0.5 Pa to 35 Pa. The increased internal pressure accelerates airflow toward the engine room outlet through the louvre system located in the upper section of the engine room.

The increase in air velocity and airflow capacity supplied to the engine room, accompanied by a rise in internal air pressure, enhances the air exchange rate within the engine room. This improvement plays a significant role in increasing the effectiveness of heat removal from the engine room.

As shown in Figures 15 (b) and (d), the observed areas indicate a reduction in air-pocket temperatures to a range of 316.4–316.8 K (43.25–43.65 °C), demonstrating that heat is continuously transported toward the natural ventilation system. In the central region, as illustrated in Figure 15, airflow is partially obstructed, leading to localized heat accumulation at approximately 317.5 K (44.35 °C). The highest temperatures are observed near the funnel, where air temperatures exceed 320 K (46.85 °C). This heat accumulation is attributed to the confined space densely occupied by exhaust piping from both the main engine and auxiliary engines, as well as the role of this area as a channel for hot air flow toward the natural ventilation outlet.

The temperature variation within the engine room, as illustrated in Figures 15 (a) and (b), indicates that the air temperature in the Frame 16 and Frame 17 areas ranges from approximately 316 K to 317 K (42–43 °C). The airflow patterns shown in Figure 12 and the air pressure distribution in Figure 14 demonstrate that the heat evacuation achieved by Variation 1 is effective in reducing the air temperature within the engine room of the tugboat *TB Hasnur 08*. Furthermore, the air temperature distribution presented in Figure 16 (f) for Variation 1 shows that heat is successfully transported toward the natural ventilation system and discharged out of the vessel.

A comparison of the air velocity profiles and temperature profiles between Variation 1 and Variation 0 indicates that the air temperature inside the engine room of the tugboat *TB Hasnur 08* decreases to a range of 316.4–316.8 K (43.25–43.65 °C). In addition, Variation 1 demonstrates an improved capability for heat evacuation compared to the previous variation.

3.2 Result from Variation 2

The concept applied in Variation 2 is essentially the same as in Variations 0 and 1, namely the use of two air supply ducts to deliver fresh air into the engine room. In Variation 2, the airflow velocity is determined based on measurement results obtained from another tugboat within the Hasnur fleet. However, the airflow velocity applied in Variation 2 is higher than that used in Variations 0 and 1. The airflow velocity values for Variation 2 are presented in Table 8.

The increased airflow velocity, combined with a ducting cross-sectional area that still complies with the existing engine room configuration, results in the air supply capacity introduced into the engine room in the simulation. The analyzed variation indicates an estimated volumetric flow rate of approximately 64.74 m^3/s. The total air supply capacity in Variation 2 remains below the total air capacity specified in the ISO 8861 standard. A comparison between the capacity obtained from the simulation and the theoretical calculation shows a ratio of 0.748 (74.8%).

TABLE 10
AIR VELOCITY VARIATION 4

Variation 4	Supply ME P	Supply AE S	Supply ME S	Supply AE S	Add Vent P	Add Vent S
V (m/S)	26,75	20	26,75	20	1.5	1,5
A (m^2)	1,009424	0,2552	1,822912	0,28462	0,785	0,785
Q (m^3/s)	27,00	5,10	48,76	5,69	1,18	1,18

The increase in airflow velocity influences the rise in air pressure within the engine room. As shown in Figures 20 (b) and (d), the louvre areas still exhibit negative pressure, ranging from approximately −4 Pa to

−5 Pa, while the engine area experiences a pressure increase of about 97.57 Pa Higher airflow velocity leads to an increase in air pressure within the engine room. The air pressure distribution inside the engine room is illustrated in Figure 22, with pressure values ranging from −54.322 Pa to 103.08 Pa. The increase in airflow velocity results in higher pressure levels across almost the entire engine room. Nevertheless, relatively higher negative pressure is observed in the lower regions of the engine room, particularly in the space between the machinery and the deck, as well as in the exhaust area at the aft section. In the observation areas shown in Figures 20 (a), (c), and (e), where pressure values range between 15 Pa and 27 Pa, higher-pressure air is concentrated in the upper regions. This condition is attributed to a faster air exchange rate within the engine room.

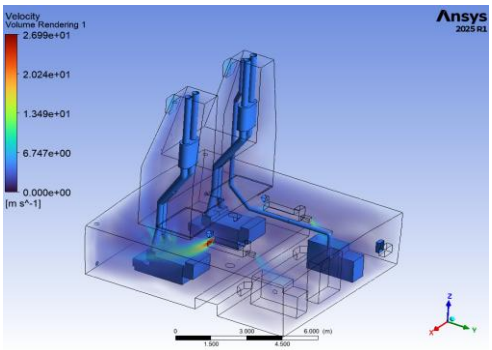

Figure 30 Air speed inside engine room Variation 4

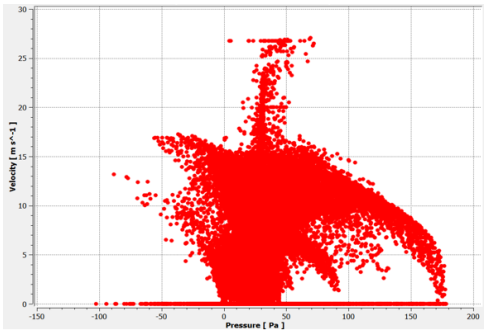

Figure 34 Air velocity and pressure chart Variation 4

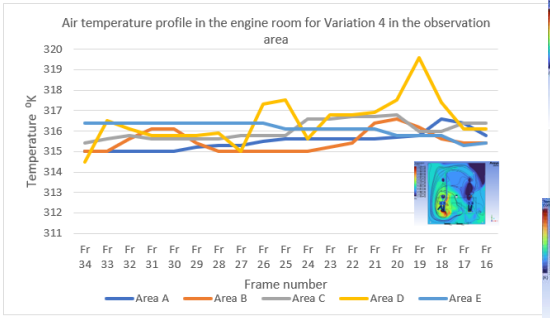

Figure 35 Temperature observation at frame Variation 4

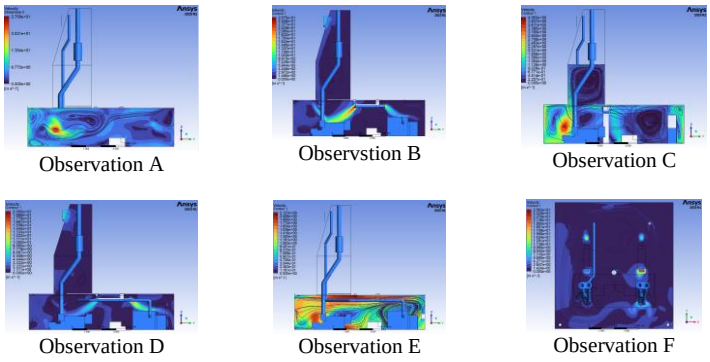

Figure 31 Air velocity at observation area Variation 4

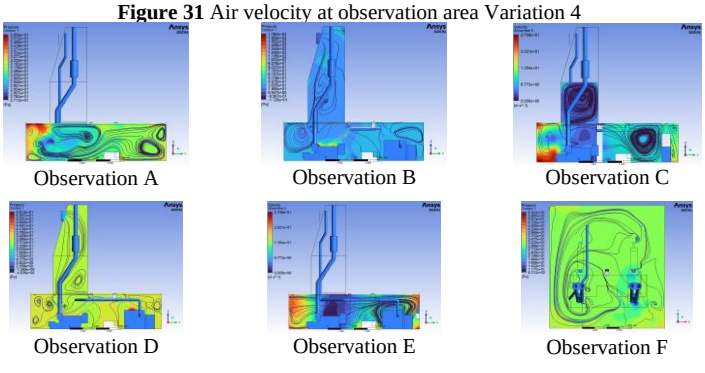

Figure 32 Pressure at observation area Varition 4

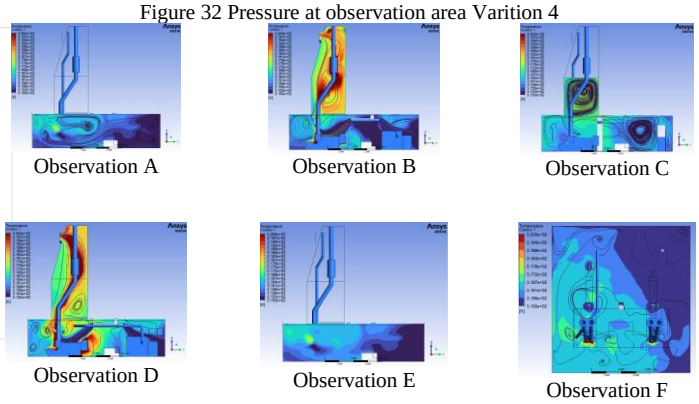

Figure 33 Temperature at observation area Variasi 4

The highest pressure recorded in Variation 2 reaches 102 Pa, while the average lowest pressure is approximately −20 Pa. This pressure differential reflects variations in airflow and pressure dynamics within the engine room in relation to the conditions of incoming and outgoing air through the ventilation pathways.

pressure in these regions increases to between 50 and 52 Pa. In observation area B (Fig 26 b), the highest air pressure is observed at the impingement zone between the airflow and the machinery, reaching a value of approximately 192 Pa.

Based on the interpretation of Figure 28, the highest air pressure within the engine room reaches up to 197 Pa, while the average air pressure throughout the engine room operates within the range of 0–110 Pa. It can therefore be concluded that the air pressure inside the engine room in this variation increases to a higher level compared to the previous variations.

With the airflow velocity determined in accordance with the ISO standard, the thermal distribution inside the engine room is shown in Figure 27. In Figure 27 (a), observation area A at the right-side wall exhibits an average temperature of approximately 315 K (41.85 °C). In Figures 27 (b) (d), corresponding to the air pocket observation areas at frames 16 and 17, the air temperature decreases to about 315 K (41.85 °C) on the right side and 316.1 K (42.95 °C) on the left side. In the central region shown in Figure 27 (c), the air temperature

in the upper zone reaches approximately 316.7 K (43.55 °C).

As illustrated in Figure 27 (f), the air temperature in observation area F averages below 316.5 K (43.35 °C). In general, the air temperature inside the engine room decreases when the air supply rate complies with the ISO 8861 standard. The lowest temperature observed in this simulation is approximately 315 K (41.85 °C) in the designated observation area.

This condition is attributed to the simulation design, in which the ambient intake air temperature is set at 309.65 K (36.5 °C), and the air entering the engine room reaches approximately 312.65 K (39.5 °C). Under these conditions, the average air temperature increase within the engine room is about 2.35 °C. Variation 3 demonstrates the most effective thermal performance among all configurations because the supplied airflow velocity complies with the ISO 8861 requirement, ensuring adequate combustion air and sufficient heat evacuation. The increased airflow momentum enhances mixing and promotes a more uniform temperature distribution throughout the engine room, thereby reducing localized heat accumulation near major heat sources such as the main engine and turbocharger region. CFD results indicate that the higher inlet velocity improves convective heat transfer, allowing hot air to be transported more efficiently toward the exhaust outlets. In addition, the balanced supply–exhaust interaction minimizes stagnant zones and weak recirculation regions that previously contributed to thermal stratification under existing conditions. As a result, the engine room temperature decreases significantly and remains more stable. These findings confirm that compliance with ISO 8861 airflow criteria is critical not only for combustion air sufficiency but also for overall thermal management and ventilation effectiveness in marine engine rooms, as the simulation is configured according to the temperature of the supplied air entering the engine room. The ambient supply air temperature is set at 309.65 K (36.5 °C), while the air entering the engine room ranges between approximately 311.65 K and 312.65 K (38.5–39.5 °C).

3.4 Result from Variation 4

The total air supplied into the engine room in the Variation 4 simulation corresponds to the air supply capacity specified in the ISO 8861 standard, amounting to 86.56 m³/s. Meanwhile, the additional exhaust functions to extract air from the engine room and is therefore represented as a negative flow rate of −2.36 m³/s, indicating the removal of air from the engine room.

The reduction in air volume, intended to facilitate the removal of heat-laden air from the aft section of the engine room on both the port and starboard sides as well as the lower region at frames 16 and 17, results in a decrease in air pressure within the engine room. The air pressure distribution inside the engine room is shown in Figure 34 (b) and (d), where the pressure around the louvre areas ranges from approximately −11 Pa to −7 Pa. In Figure 334 (c), the pressure in the lower central region increases due to the suction effect generated by the exhaust ducts, with the air pressure in this area reaching approximately 27 Pa.

In the observation areas at the lower right-side wall, the central region Figure 32(c), and the lower left-side wall of the engine room, an increase in air pressure is observed due to the presence of exhaust ducts installed in the lower part of the engine room. Conversely, pressure readings at the upper natural ventilation louvre areas show a decrease, as a portion of the air pressure is drawn toward the exhaust outlets located in the lower section of the engine room.

Figure 34 shows that the air pressure inside the engine room ranges from −100 Pa to 180 Pa. The maximum pressure observed in Variation 4 decreases compared to the previous variation, as a portion of the air capacity is reduced through the exhaust outlets.

Based on the temperature observations shown in Figure 33 (f), the heat extracted through the exhaust pipe increases to approximately 319 K (45.85 °C). In addition, the temperature in the funnel area, as illustrated in Figures 35 (b) and (d), also increases. This behavior is attributed to the reduction in air pressure, which causes the heat in this region in Variation 3 to be transported upward toward the louvre more slowly.

The exhaust installed in the lower section of the engine room can be considered sufficiently effective in extracting heat from the hot air pocket regions at frames 16 and 17, where the temperatures are approximately 316.4 K (43.25 °C) and 316.8 K (43.25 °C), respectively. However, it also results in a reduction of air temperature in the central region. As observed in the area near the exhaust duct, the air temperature is lower, at about 315.4 K (42.25 °C). This condition occurs because the airflow has not fully absorbed heat before being drawn out by the exhaust system.

Observations in the hot air pocket regions under Variation 4 indicate a reduction in temperature within the engine room. However, when compared to Variation 3, the temperatures in Variation 4 are higher by approximately 0.2–0.3 °C. Nevertheless, at frame 19, a temperature increase of about 3 °C is observed, which is attributed to a reduction in air pressure in this area.

Variation 4 applies the same airflow velocity as Variation 3 but introduces an additional exhaust duct at Frame 16/17 to enhance hot air extraction from the upper region. The CFD analysis shows that this modification improves localized heat removal and reduces hot air accumulation near the deck–bulkhead intersection, where thermal stratification typically occurs. However, the overall temperature reduction is slightly less effective than Variation 3 due to changes in airflow distribution. The additional exhaust path alters the pressure balance and redistributes airflow, causing part of the incoming air to be diverted before fully sweeping major heat-generating zones. Consequently, although localized ventilation improves, the global convective heat transfer is not as uniform as in Variation 3. This indicates that exhaust placement must be carefully balanced with supply airflow to avoid short-circuiting effects. Nonetheless, Variation 4 remains effective in improving thermal comfort and reducing localized overheating,

particularly in the upper engine room region prone to hot air entrapment.

IV. CONCLUSION

This study aimed to design, evaluate, and validate an optimal engine room ventilation model for the TB Hasnur 08 tugboat in accordance with ISO 8861 standards using Computational Fluid Dynamics (CFD). The results demonstrate that ventilation performance is strongly influenced by airflow capacity, velocity, and duct configuration, which directly affect temperature distribution and heat removal within the engine room. Under existing conditions, significant heat accumulation was observed, leading to relatively high engine room temperatures. The implementation of improved ventilation configurations successfully reduced the temperature and enhanced airflow distribution.

Among the evaluated configurations, Variation 3, which applies airflow velocity in compliance with ISO 8861, provided the most effective temperature reduction and overall ventilation performance. This configuration achieved better heat evacuation and minimized hot air accumulation compared to other variations. The study also confirms that CFD is a reliable and effective tool for predicting thermal behavior and airflow patterns in marine engine rooms, enabling systematic evaluation and optimization of ventilation system design. Therefore, the proposed ventilation approach can improve thermal conditions, operational safety, and machinery reliability in tugboat engine rooms.

ACKNOWLEDGEMENTS

The author sincerely thanks my family and the entire TB Hasnur 08 crew who assisted with this research, the Hasnur team, and friends who could not be named individually. I also extend thanks to the individuals and institutions who provided support throughout this research. Their contributions, whether direct or indirect, were invaluable in completing this work

REFERENCES

[1] Alizadeh, E., A. Maleki, and A. Mohamadi, *An investigation of the effect of ventilation inlet and outlet arrangement on heat concentration in a ship engine room.* Engineering, Technology & Applied Science Research, 2017. **7**(5): p. 1996-2004.

[2] Alsaad, H. and C. Voelker, Performance assessment of a ductless personalized ventilation system using a validated CFD model. Journal of Building Performance Simulation, 2018. 11(6): p. 689-704.

[3] Mollenhauer, K., H. Tschöke, and K.G.E. Johnson, *Handbook of diesel engines*. Vol. 1. 2010: Springer Berlin.

[4] Hendri, N.S., O.S. Ahmadi, and A.D. Susanto, *The Air Flow Analysis in Engine Rooms at Frigate Class Ship with CFD Approach (Computational Fluids Dynamics).* Int. J. Recent Eng. Sci, 2018. **5**: p. 11-18.

[5] *Moerdjoko, M., KAITAN SISTEM VENTILASI BANGUNAN DENGAN KEBERADAAN MIKROORGANISME UDARA. DIMENSI (Journal of Architecture and Built Environment), 2004. 32(1).*

[6] He, M., et al. *Design and Research of Marine Nuclear Power Platform Engine Room Ventilation System*. in *IOP Conference Series: Earth and Environmental Science*. 2020. IOP Publishing.

[7] Dewi, F.G.U., *Pengaruh Kecepatan Dan Arah Aliran Udara Terhadap Kondisi Udara Dalam Ruangan Pada Sistem Ventilasi Alamiah.* Rekayasa Mesin, 2012. **3**(2): p. 299-304.

[8] Setiawan, F.A., S.P. Fitri, and D.I.A. Santoso, *Simulasi CFD Sistem Ventilasi dan Pengaturan Udara Ruangan Isolasi Covid-19 di Kapal Perintis 750 DWT.* 2021.

[9] Newton, W., et al., *Investigating the thermal profile of a marine vessel engine room through simulation with field measurements.* Applied Thermal Engineering, 2014. **73**(1): p. 1360-1370.

[10] Caterpillar, *Application & Installation Guide Engine Room Ventilation*. 2015: CAT. 36.

[11] Pérez, J.A., J.A. Orosa, and Á.M. Costa, *Energetic optimization of the ventilation system in modern ships.* Applied Thermal Engineering, 2016. **108**: p. 816-823 %@ 1359-4311.

[12] Orosa, J.A., Á.M. Costa, and J.A. Pérez, *A new modelling procedure of the engine room ventilation system for work risk prevention and energy saving.* Proceedings of the Institution of Mechanical Engineers, Part M: Journal of Engineering for the Maritime Environment, 2017. **231**(4): p. 863-870 %@ 1475-0902.

[13] MAN, ence of ambient temperature conditions on main engine operation of B&W two-strokeengines. 2014. CLassNK, *RULES FOR THE SURVEY AND CONSTRUCTION OF STEEL SHIPS Part DMACHINERY INSTALLATIONS*. 2024.

[14] Balakrishnan, P.K.S. and S. Sasi. *Technological and Economic Advancement of Tug Boats*. 2016.

[15] Beegle, R., *An Overview of Trends in the Tug Marked.* Marcon International, Inc, 2007.

[16] Hubla, D.p.l., *Pengembangan E-Book Data dan Penyajian Informasi Angkutan Laut "Data dan informasi angkutan laut 2020"*. 2020.

[17] Nowruzi, H. and A. Najafi, *An experimental and CFD study on the effects of different pre-swirl ducts on propulsion performance of series 60 ship.* Ocean Engineering, 2019. **173**: p. 491-509.

[18] Susilo, J., A. Santoso, and T.B. Musyiradi, *Simulasi Penggunaan Fin Undership Terhadap Tahanan dan Gaya Dorong Kapal dengan Metode Analisa CFD.* Jurnal Teknik ITS, 2014. **3**(2): p. G174-G179.

[19] Mulyadi, M., *Analisis Aerodinamika pada Sayap Pesawat Terbang dengan Menggunakan Software Berbasis Computational Fluid Dynamics (CFD).* Universitas Gunadarma, Depok, 2010.

[20] Mulyadi, M., *Analisis Aerodinamika pada Sayap Pesawat Terbang dengan Menggunakan Software Berbasis Computational Fluid Dynamics (CFD).* Universitas Gunadarma, Depok, 2010.

[21] Nugroho, A., W.A. Widodo, and I.B. Suryo. *Numerical study of engine room air ventilation systems for landing ship tank class warships in supporting crew comfort and safety*. IOP Publishing.

[22] Gilbert Gedeon, P.E., *Diesel Engine Fundamentals.* New York: CED, 2009.

[23] Es-sakali, N., et al., *Review of predictive maintenance algorithms applied to HVAC systems.* Energy Reports, 2022. **8**: p. 1003-1012. ESDM, *Road Map Pengembangan dan Pemanfaatan Batubara 2021 - 2045*. 2021.